

Supporting Information for

Revisiting the BaO₂/BaO redox cycle for solar thermochemical energy storage

*Alfonso J. Carrillo[†], Daniel Sastre[†], David P. Serrano^{†, ‡}, Patricia Pizarro^{†, ‡, *} and Juan M.*

Coronado[†]

[†]Thermochemical Processes Unit, IMDEA Energy Institute, Avenida Ramón de la Sagra, 3,
Parque Tecnológico de Móstoles, 28935, Móstoles, Madrid, Spain.

[‡]Chemical and Environmental Engineering Group, ESCET, Rey Juan Carlos University, c/
Tulipán s/n, 28933, Móstoles, Madrid, Spain.

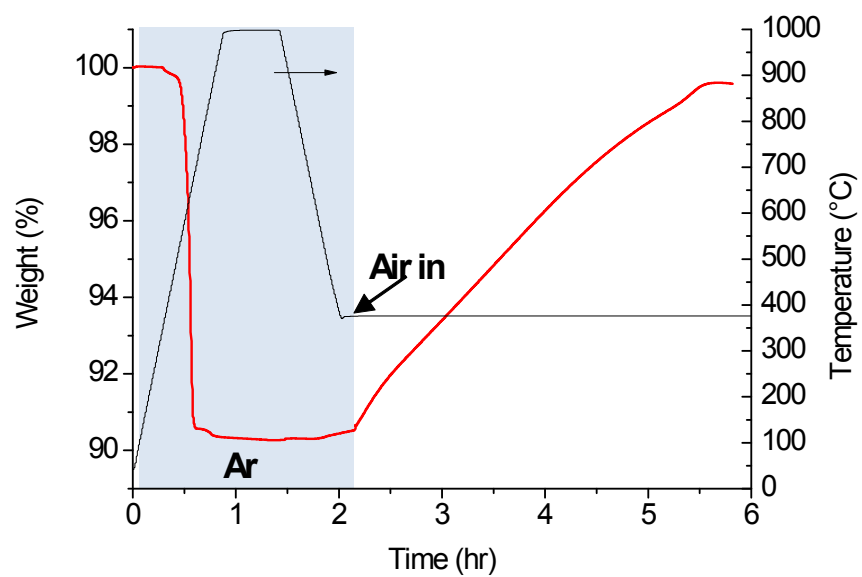


Figure S1. Example of a TGA run carried out to extract oxidation kinetic data.

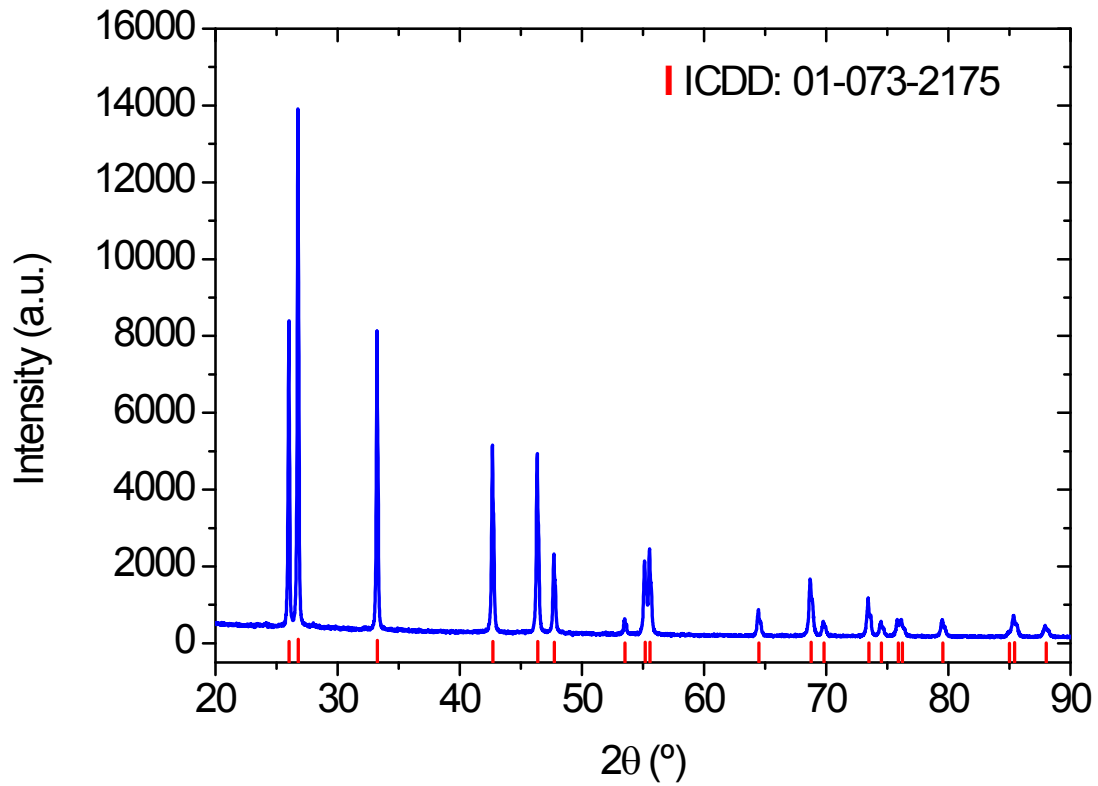


Figure S2. XRD pattern of BaO₂ commercial sample.

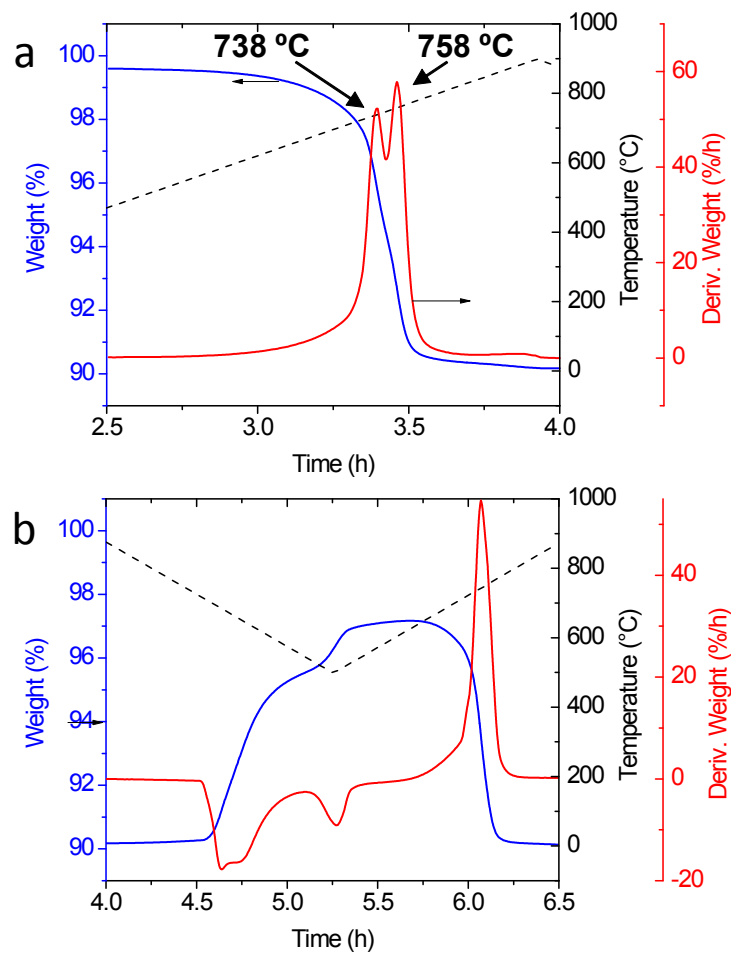


Figure S3. Derivative of weight for (a) reduction step in the first cycle and (b) oxidation step in the first cycle and reduction step in the second cycle.

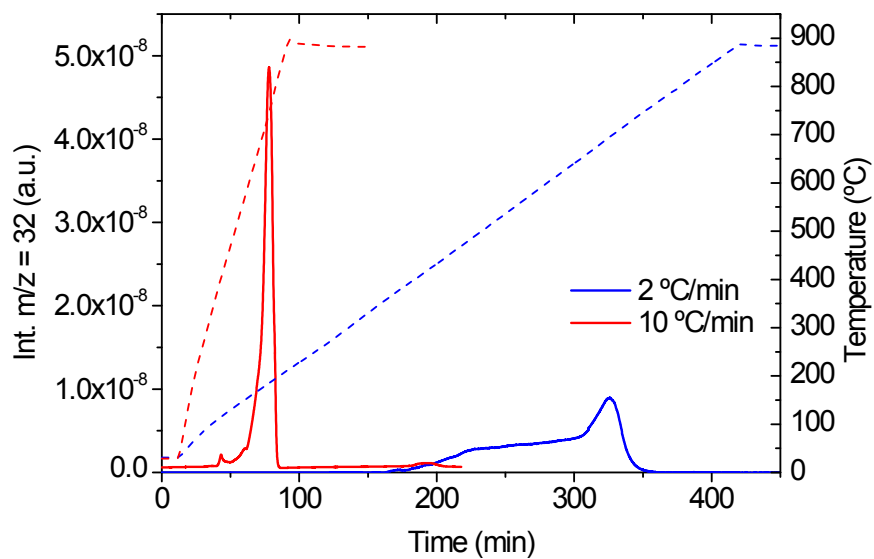


Figure S4. Comparison of the oxygen evolution during BaO₂ reduction measured by mass spectrometry for two different heating ramps. Reduction was performed under a constant Ar flow of 50 ml min⁻¹.

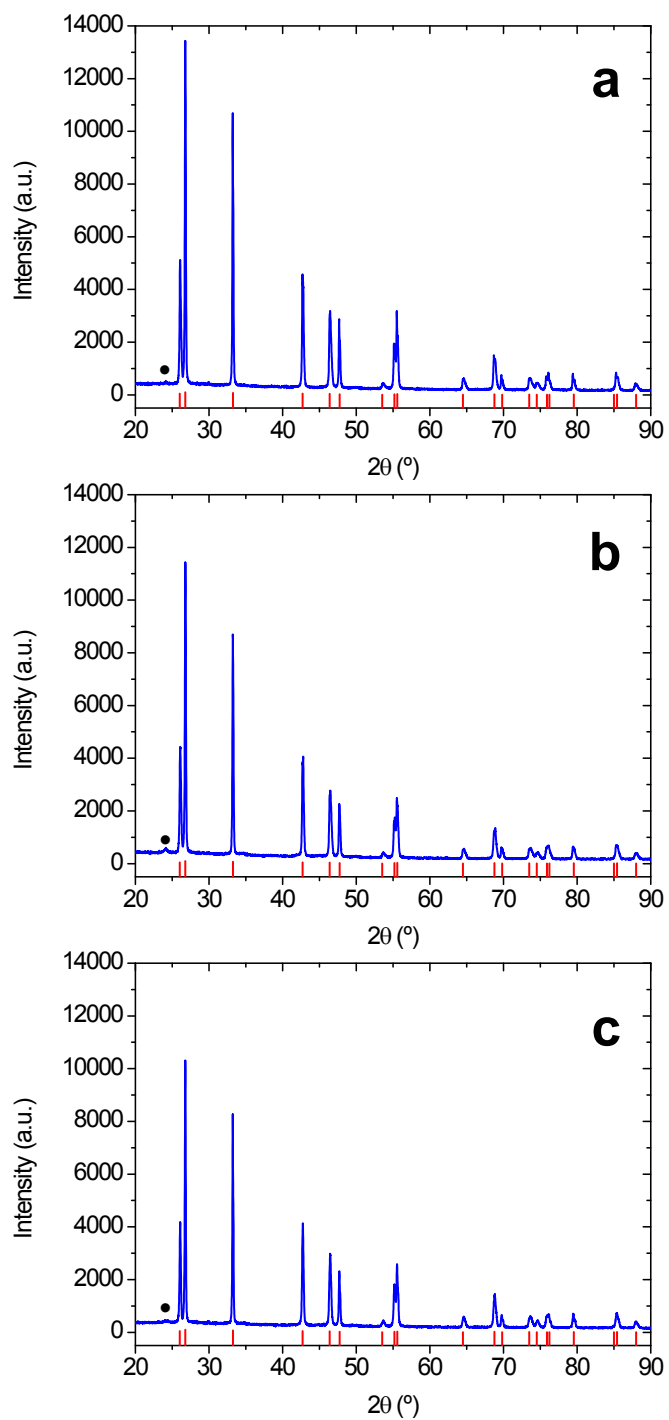


Figure S5. XRD patterns after 10 redox cycles using cooling rates of (a) $10\text{ }^{\circ}\text{C min}^{-1}$, (b) $5\text{ }^{\circ}\text{C min}^{-1}$ and (c) $2\text{ }^{\circ}\text{C min}^{-1}$. • Unknown phase, | BaO_2 .

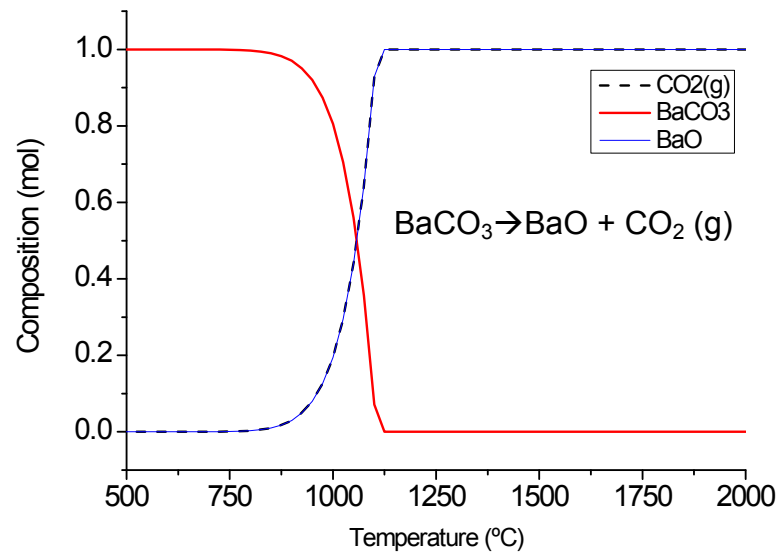


Figure S6. BaCO₃ decomposition simulated with HSC software.

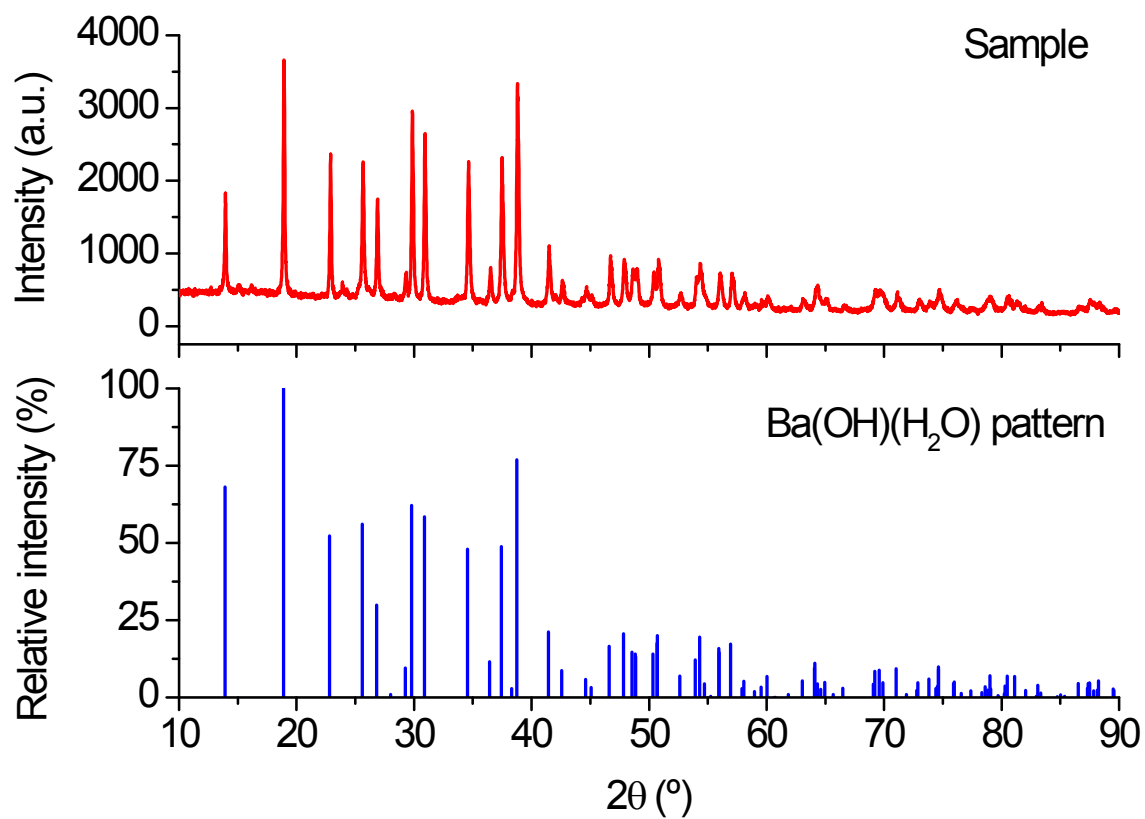


Figure S7. XRD analysis of BaO₂ sample after reduction and exposure to ambient moisture, presenting Ba(OH)(H₂O) crystal phase.

SI-A Master plot construction

The rate of a solid-state reaction can be described as:

$$\frac{d\alpha}{dt} = A \exp\left(-\frac{E_a}{RT}\right) f(\alpha) \quad (\text{S1})$$

Where α the conversion fraction, A is the pre-exponential factor; E_a , is the activation energy, R the gas constant and $f(\alpha)$ the reaction model. The most representative models for solid-state reactions are shown on Table S1. As TGA is used to study the reaction, α is defined by

$$\alpha = \frac{m_0 - m_t}{m_0 - m_f} \quad (\text{S2})$$

where m_0 is initial weight, m_t is weight at time t and m_f is final weight.

By integrating Eq. S2 under isothermal conditions it is obtained the integral form of the kinetic rate law:

$$g(\alpha) = A \exp\left(-\frac{E_a}{RT}\right) t \quad (\text{S3})$$

For the master plot construction [S1,S2,S3], it is necessary to introduce the generalized time θ [S4]:

$$\theta = \int_0^t \exp\left(-\frac{E_a}{RT}\right) dt = \exp\left(-\frac{E_a}{RT}\right) t \quad (\text{S4})$$

Combining Eqs. S4 and S5 results in:

$$g(\alpha) = A\theta \quad (\text{S5})$$

From Eq. S6 and taking as reference point $\alpha = 0.5$ [S1] it is obtained:

$$\frac{g(\alpha)}{g(0.5)} = \frac{\theta}{\theta_{0.5}} \quad (\text{S6})$$

where $\theta_{0.5}$ is the generalized time at $\alpha = 0.5$. Then, by plotting $g(\alpha)/g(\alpha_{0.5})$ against α for the most common kinetics models in solid-state reactions (Table S1) the theoretical master plot based on

the integral form of the kinetic data is constructed (Figure S12) . It can be appreciated that all the plots coincide at $\alpha = 0.5$. As the kinetic analysis is carried out under isothermal conditions, the exponential term in Eq. S5 is constant. Then it can be established that:

$$\frac{g(\alpha)}{g(0.5)} = \frac{t}{t_{0.5}} \quad (\text{S8})$$

By representing $t/t_{0.5}$, experimental data obtained by TGA, against α and comparing it with the theoretical master plot curves it will be possible to discern the kinetic model of the reaction.

References

S1-F.J. Gotor, J.M. Criado, J. Malek, N. Koga, The Journal of Physical Chemistry A. 104 (2000) 10777–10782.

S2-P.E. Sánchez-Jiménez, L.A. Pérez-Maqueda, A. Perejón, J.M. Criado, J. Phys. Chem. A 114 (2010) 7868.

S3-P.E. Sánchez-Jiménez, L.A. Pérez-Maqueda, A. Perejón, J.M. Criado, Thermochim. Acta 552 (2013) 54.

S4-T. Ozawa, Thermochim. Acta 100 (1986) 109.

Table S1. Representative gas-solid kinetic models used in this work.

Model		$f(\alpha)$	$g(\alpha)$
<i>Reaction-order models</i>			
Zero-order	(F0/R1)	1	α
First-order	(F1)	$(1-\alpha)$	$-\ln(1-\alpha)$
Second-order	(F2)	$(1-\alpha)^2$	$(1-\alpha)^{-1}-1$
Third-order	(F3)	$(1-\alpha)^3$	$0.5[(1-\alpha)^{-2}-1]$
<i>Nucleation models</i>			
Power law	(P2)	$2\alpha^{1/2}$	$\alpha^{1/2}$
Power law	(P3)	$3\alpha^{2/3}$	$\alpha^{1/3}$
Power law	(P4)	$4\alpha^{3/4}$	$\alpha^{1/4}$
Avrami-Erofeev	(A2)	$2(1-\alpha)[-\ln(1-\alpha)]^{1/2}$	$[-\ln(1-\alpha)]^{1/2}$
Avrami-Erofeev	(A3)	$3(1-\alpha)[-\ln(1-\alpha)]^{2/3}$	$[-\ln(1-\alpha)]^{1/3}$
Avrami-Erofeev	(A4)	$4(1-\alpha)[-\ln(1-\alpha)]^{3/4}$	$[-\ln(1-\alpha)]^{1/4}$
<i>Contraction models</i>			
Contracting area	(R2)	$2(1-\alpha)^{1/2}$	$[1-\ln(1-\alpha)]^{1/2}$
Contracting volume	(R3)	$3(1-\alpha)^{2/3}$	$[1-\ln(1-\alpha)]^{1/3}$
<i>Diffusion models</i>			
1D Diffusion	(D1)	$1/2\alpha$	α^2
2D Diffusion	(D2)	$[-\ln(1-\alpha)]^{-1}$	$[(1-\alpha)\ln(1-\alpha)]+\alpha$
3D Diffusion-Jander Eq.	(D3)	$3(1-\alpha)^{2/3}/2(1-(1-\alpha)^{1/3})$	$[1-(1-\alpha)^{1/3}]^2$
Ginstling-Brounshtein	(D4)	$(3/2)((1-\alpha)^{-1/3}-1)$	$1-(2\alpha/3)-(1-\alpha)^{2/3}$

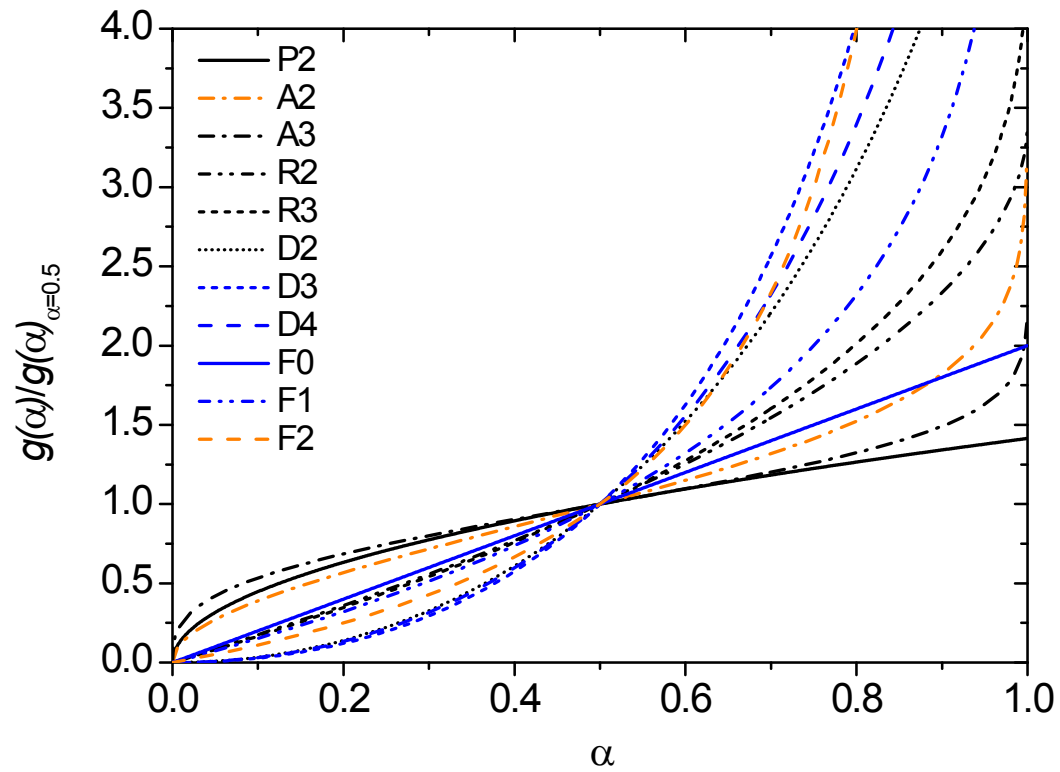


Figure S8. Theoretical master plot curves in integral form representing $g(\alpha)/g(0.5)$ as a function of α for the different kinetic models.